Periplaneta americana extract ameliorates lipopolysaccharide-induced liver injury by improving mitochondrial dysfunction via the AMPK/PGC-1α signaling pathway

WEI SHI, LI AN, JUN ZHANG and JIE LI

Department of Geriatrics, Zhongda Hospital, School of Medicine, Southeast University, Nanjing, Jiangsu 210009, P.R. China

Received April 1, 2021; Accepted July 8, 2021

DOI: 10.3892/etm.2021.10572

Abstract. *Periplaneta americana* (PA) extract acts clinically as a therapeutic treatment in various diseases; it enhances liver function in mouse models and mitigates the pathological condition of liver fibrosis. The present study aimed to investigate the role and potential mechanisms underlying the action of the PA extract, xinmailong (XML), in lipopolysaccharide (LPS)-induced liver injury. Following the treatment of AML12 cells with LPS, the content of cytochrome *c* in the cytoplasm and mitochondria, and the level of ATP synthesis were detected using corresponding kits. The relative mRNA expression levels of nuclear respiratory factor 1 and transcription factor A, mitochondrial were investigated using reverse transcription-quantitative (RT-q)PCR analysis. The MTT assay was performed to detect the viability of AML12 cells following treatment with XML, in the absence or presence of LPS. Western blot analysis was performed to determine the expression levels of proteins in the AMP-activated protein kinase (AMPK)/proliferator-activated receptor γ coactivator-1α (PGC-1α) pathway. Following treatment with compound C, an inhibitor of AMPK, the expression levels of inflammatory cytokines were determined using ELISA and RT-qPCR analysis. The levels of oxidative stress-related markers were detected using corresponding kits following treatment with compound C. In addition, TUNEL staining was performed to detect the apoptosis of AML12 cells, and western blot analysis was performed to investigate the expression levels of apoptosis-related proteins. Mitochondrial dysfunction was induced by LPS in AML12 cells. LPS stimulation significantly downregulated the expression of proteins in the AMPK/PGC-1α pathway, which was reversed following treatment with XML. In addition, inflammation, oxidative stress and mitochondrial dysfunction induced by LPS were alleviated by XML in AML12 cells. However, the addition of compound C and XML to LPS-induced AML12 cells resulted in the aggravation of cell injury. Collectively, the results of the present study indicated that XML suppressed mitochondrial dysfunction induced by LPS by activating AMPK/PGC-1α signaling. Thus, the results of the present study may contribute to further understanding of the underlying mechanism via which XML alleviates liver injury.

Correspondence to: Dr Jie Li, Department of Geriatrics, Zhongda Hospital, School of Medicine, Southeast University, 87 Dingjiaqiao Road, Nanjing, Jiangsu 210009, P.R. China
E-mail: lijiejjj2020@163.com

Key words: liver injury, lipopolysaccharide, mitochondrial dysfunction, inflammation, AMP-activated protein kinase

Introduction

The liver performs and regulates numerous physiological functions, and has the ability to regenerate (1,2). It is an important line of defense against microorganisms and is also a target of the dysregulated inflammation induced by infectious diseases of the liver such as steatohepatitis (3). Based on the International Classification of Diseases, Ninth Revision, Clinical Modification, severe sepsis and septic shock are main causes for hospital patients to be admitted to intensive care unit (4). Sepsis is defined as a life-threatening organ dysfunction caused by a dysregulated host response to infection (5). Among the organ failures involved in sepsis, hepatic dysfunction has a high level of prognostic relevance for the course of sepsis and is a powerful independent predictor of mortality (6).

The *Periplaneta americana* (PA) extract is found in the American cockroach and comprises polyols, peptides, epidermal growth factors, sticky sugar acid, amino acids and further active components (7). The PA extract notably alleviates swelling of liver tissue and stomach pain in gastric ulcer (8,9). Furthermore, it is widely used in China for its beneficial effects on blood circulation, hematocele clearance and digestion (10). Xinmailong (XML), which is typically made from PA, reverses the cardiomyocyte damage caused by lipopolysaccharide (LPS) by mediating mitophagy and downregulating the expression of inflammatory factors (11). PA extract protected the intestinal mucosal barrier in patients with sepsis, thereby improving the physical condition of the patients and ameliorating prognosis (7). PA extract reduced the level

of endotoxin, attenuated gastrointestinal complications, and improved immune function and nutritional status in patients with systemic inflammatory response syndrome (7,12). The results of a previous study demonstrated that XML alleviated intestinal inflammation and improved the intestinal mucosal barrier function (10). By decreasing the expression levels of fibrosis-related genes, the liver function of mice was enhanced, and the pathological fibrosis associated with liver were mitigated or even reversed, resulting in inhibition of liver fibrosis progression (13). Additionally, PA extract accelerated liver regeneration via a complex network of pathways, including AMP-activated protein kinase (AMPK) signaling (14). The activation of AMPK maintained mitochondrial function and regulated autophagy, thus preventing sepsis-induced cell and organ injury (15). A previous study has proposed that inhibition of the AMPK/proliferator-activated receptor γ coactivator-1α (PGC-1α) signaling pathway in rat liver induced diseases associated with mitochondrial dynamics (16).

The present study aimed to investigate the role of XML in LPS-induced liver injury and determined whether the potential underlying mechanism is associated with regulation of the AMPK/PGC-1α signaling pathway.

Materials and methods

Cell culture and treatments. The AML12 cell line (cat. no. 3101MOUSCSP550) was purchased from The Cell Bank of Type Culture Collection of the Chinese Academy of Sciences and maintained in DMEM (Invitrogen; Thermo Fisher Scientific, Inc.) supplemented with 10% FBS (Sigma-Aldrich; Merck KGaA), 100 U/ml penicillin and 100 μg/ml streptomycin (Beyotime Institute of Biotechnology). Once cells reached 80% confluence, they were treated with 100 ng/ml LPS for 12 h at 37˚C. Certain cells were also preincubated with 0.25, 0.5, 1, 2 and 4 mg/ml of the PA extract, XML (Yunnan Tengyao Pharmaceutical, Co., Ltd.) for 48 h. Cells were treated with 2 mg/ml AMPK inhibitor, compound C (Sigma-Aldrich; Merck KGaA) for 1 h at 37˚C before model establishment.

Detection of cytochrome c. Cytochrome *c* content in the mitochondria and cytoplasm was detected using a Quantikine Mouse Cytochrome *c* Immunoassay kit obtained from R&D Systems, Inc. (cat. no. MCTC0), according to the manufacturer's protocol. The AML12 cells were lysed with lysis buffer (Beyotime Institute of Biotechnology) containing protease inhibitors (Sigma-Aldrich; Merck KGaA). The lysate was centrifuged for 10 min at 750 x g, and the supernatants were collected and subsequently centrifuged at 15,000 x g for 15 min at 4˚C. The supernatants were used as the cytosolic fractions. The pellet containing the mitochondria was combined with PBS plus 0.5% Triton X-100 (Sigma-Aldrich; Merck KGaA) for 10 min at 4˚C. The pellet was centrifuged at 15,000 x g, 4˚C for 10 min, and the supernatant was used as the mitochondrial fraction.

Luciferin-luciferase reaction. Mitochondria were collected from cells by centrifugation at 4˚C, 12,000 x g for 8 min. Then, 100 μl sample was added in a 96-well plate before 100 μl ATP reagent was added for 2 min. ATP concentration was measured using an enhanced ATP assay kit (cat. no. S0027, Beyotime Institute of Biotechnology), according to the manufacturer's protocol.

MTT assay. Cell viability was assessed using an MTT assay. Cells were seeded into 96-well plates at a density of $2x10^4$ cells/well following culture with or without XML at concentrations of 0.25, 0.5, 1, 2 and 4 mg/ml respectively for 48 h at 37˚C. The DMEM containing serum was replaced with MTT (Sigma-Aldrich; Merck KGaA) following the corresponding treatment. Subsequently, 0.5 mg/ml MTT reagent was added to each well and incubated for 4 h at 37˚C. The cell supernatant was discarded and replaced with DMSO (150 μl/well). The absorbance was measured at a wavelength of 570 nm using a microplate reader (Bio-Rad Laboratories, Inc.).

ELISA. AML12 cells were seeded into 96-well plates at a density of $1x10^5$ cells/well and co-treated with 100 ng/ml LPS, 4 mg/ml XML and 5 mM compound C for 12 h. The supernatants of the cultured cells were collected in a centrifuge at 1,000 x g, 4˚C for 15 min to measure the secretion levels of IL-1β (cat. no. F10770), IL-6 (cat. no. F10830) and TNF-α (cat. no. F11630) using commercial ELISA kits, according to the manufacturer's protocol (Shanghai Xitang Biological Technology Co., Ltd.).

Measurement of oxidative stress-related markers. The cell malondialdehyde (MDA; cat. no. A003-4-1) assay kit and total superoxide dismutase (SOD; cat. no. A001-1-2) assay kit were purchased from Nanjing Jiancheng Bioengineering Institute. The measurement of MDA and SOD was performed according to the manufacturer's protocol.

TUNEL assay. Apoptosis of AML12 cells was detected using a TUNEL assay kit (Beyotime Institute of Biotechnology), according to the manufacturer's protocol. Briefly, $2x10^5$ cells were washed twice with buffer in 24-well plates and then fixed in 0.5 ml 4% paraformaldehyde for 30 min at 37˚C. Subsequently, cells were incubated with 50 μl TUNEL reaction buffer for 1 h at 37˚C. The nuclei were counterstained with 1 μg/ml DAPI in the dark at room temperature for 15 min. Images were visualized and captured using a fluorescence microscope (magnification, x200; Olympus Corporation) and cells were counted in five randomly-selected microscopic fields.

Reverse transcription-quantitative (RT-q)PCR. Total RNA was isolated from AML12 cells using TRIzol® reagent (Thermo Fisher Scientific, Inc.). Total RNA was reverse transcribed into cDNA using a SuperScript™ IV First-Strand Synthesis system (Invitrogen; Thermo Fisher Scientific, Inc.) according to the manufacturers' protocol. qPCR was subsequently performed using the SYBR Green PCR system and SYBR Green reagents (Bio-Rad Laboratories, Inc.) in an ABI 7500 thermal cycler (Applied Biosystems; Thermo Fisher Scientific, Inc.). The following thermocycling conditions were used for qPCR: Initial denaturation at 95˚C for 3 min, followed by 40 cycles of denaturation at 95˚C for 10 sec, annealing at 60˚C for 5 sec and extension at 72˚C for 10 sec. The sequences of the primers were as follows: NRF1 forward, 5'-CGCAGC

ACCTTTGGAGAA-3' and reverse, 5'-CCCGACCTGTGG AATACTTG-3'; TFAM forward, 5'-GGAATGTGGAGCGTG CTAAA-3' and reverse, 5'-TGCTGGAAAAACACTTCG GAATA-3'; TNF-α forward, 5'-CGTGCTCCTCACCCACAC -3' and reverse, 5'-GGGTTCATACCAGGGTTTGA-3'; IL-6 forward, 5'-ACAACCACGGCCTTCCCTACTT-3' and reverse, 5'-GTGTAATTAAGCCTCCGACT-3'; IL-1β forward, 5'-TCC AGGATGAGGACATGAGCAC-3' and reverse, 5'-GAACGT CACACACCAGCAGGTA-3' and GAPDH forward, 5'-TCA CCACCATGGAGAAGGC-3' and reverse, 5'-GCTAAGCAG TTGGTGGTGCA-3'. GAPDH was used for normalization of mRNA levels. Relative mRNA expression levels were calculated using the $2^{-\Delta\Delta Cq}$ method (17).

Western blotting. Following treatment, protein samples were extracted from cells using RIPA lysis buffer (Beyotime Institute of Biotechnology) for western blot analysis. A BCA Protein Assay kit (Beyotime Institute of Biotechnology) was used to determine total protein concentrations. Proteins (40 μg/lane) were separated via 10 or 12.5% SDS-PAGE, transferred onto PVDF membranes (MilliporeSigma) and blocked with 5% non-fat milk for 2 h at room temperature. The membranes were washed three times with 1% TBS-Tween-20 and incubated with primary antibodies overnight at 4˚C. Following the primary incubation, membranes were incubated with goat anti-rabbit horseradish peroxidase (HRP)-conjugated secondary antibody (cat. no. 7074S, 1:2,000; Cell Signaling Technology, Inc.) or horse anti-mouse HRP-conjugated secondary antibody (cat. no. 7076S, 1:2,000; Cell Signaling Technology, Inc.) for 1 h at room temperature. Protein bands were developed using an Enhanced Chemiluminescence Western Blotting Substrate kit (Thermo Fisher Scientific, Inc.). The primary antibodies used were as follows: Anti-phosphorylated (p)-AMPK (cat. no. 2535T, 1:1,000; Cell Signaling Technology, Inc.); anti-AMPK (cat. no. 5831T, 1:1,000; Cell Signaling Technology, Inc.); anti-PGC-1α (cat. no. 2178S, 1:1,000; Cell Signaling Technology, Inc.); anti-Bcl-2 (cat. no. 3498T, 1:1,000; Cell Signaling Technology, Inc.); anti-cleaved caspase-3 (cat. no. 9664T, 1:1,000; Cell Signaling Technology, Inc.); anti-caspase-3 (cat. no. 14220T, 1:1,000; Cell Signaling Technology, Inc.); anti-cleaved caspase-9 (cat. no. 20750S, 1:1,000; Cell Signaling Technology, Inc.); anti-caspase-9 (cat. no. 9508T, 1:1,000; Cell Signaling Technology, Inc.); anti-Bax (cat. no. ab182733, 1:2,000; Abcam) and anti-GAPDH (cat. no. 5174T, 1:1,000; Cell Signaling Technology, Inc.). The grayscale values of the membranes were semi-quantified using ImageJ software (version 1.52r; National Institutes of Health). Protein levels were normalized to GAPDH.

Bioinformatics. Kyoto Encyclopedia of Genes and Genomes was used to analyze the signalling pathways involved in AMPK (genome.ad.jp/kegg/).

Statistical analysis. Statistical analysis was performed using GraphPad Prism (version 8.0.1; GraphPad Software, Inc.). All experiments were repeated three times and data are presented as the mean ± standard deviation. An unpaired Student's t-test was used to compare differences between two groups, while one-way analysis of variance (ANOVA) followed by Tukey's post hoc test was used to compare differences between multiple groups. $P<0.05$ was considered to indicate a statistically significant difference.

Results

LPS induces mitochondrial dysfunction in AML12 cells. To establish the sepsis-induced liver injury model, LPS was used to induce AML12 cells. As presented in Fig. 1A and B, the level of mitochondrial cytochrome *c* significantly decreased compared with the control group, while that of cytosolic cytochrome *c* significantly increased, following LPS induction. Furthermore, ATP synthesis significantly decreased following LPS stimulation compared with the untreated group (Fig. 1C). The relative mRNA expression levels of nuclear respiratory factor 1 (NRF1) and transcription factor A, mitochondrial (TFAM) were detected via RT-qPCR analysis, and their expression levels were significantly decreased following treatment of AML12 cells with LPS compared with the group without LPS (Fig. 1D and E). Oxidative stress and reduction in ATP production are involved in mitochondrial dysfunction, and along with apoptosis, are key factors for the occurrence of acute liver injury caused by sepsis (18). Collectively, these results suggested that LPS induced mitochondrial dysfunction in AML12 cells.

XML treatment activates the AMPK/PGC-1α signaling pathway. Kyoto Encyclopedia of Genes and Genomes analysis demonstrated that mitochondrial function can be mediated by the AMPK/PGC-1α signaling pathway; thus, the effect of XML on this pathway was investigated in the present study. AML12 cells were treated with a range of concentrations of XML (0-4 mg/ml), and no significant differences in cell viability were observed (Fig. 2A). Furthermore, the viability of AML12 cells induced by LPS was detected via the MTT assay. The viability of LPS-induced AML12 cells was significantly decreased compared with the untreated group; however, cell viability increased following treatment with XML in a concentration-dependent manner; furthermore, the results showed a significant increase in cell viability compared with the LPS group following 2 and 4 mg/ml XML treatment (Fig. 2B). Therefore, 4 mg/ml XML was used for subsequent experiments. The expression levels of the proteins in the AMPK/PGC-1α signaling pathway were detected using western blot analysis. The expression levels of p-AMPK and PGC-1α were significantly decreased following LPS stimulation compared with the control group, the effects of which were reversed following 4 mg/ml XML intervention (Fig. 2C), suggesting that XML may activate the AMPK/PGC-1α signaling pathway in LPS-induced AML12 cells.

XML treatment suppresses LPS-induced inflammation, oxidative stress and apoptosis by activating AMPK/PGC-1α signaling in AML12 cells. To determine the potential mechanism via which XML exerts its effects on LPS-induced AML12 cell injury, the AMPK inhibitor compound C (2 mg/ml) was used for pretreatment together with 4 mg/ml XML in LPS-induced AML12 cells. The levels of inflammatory factors were detected using ELISA and RT-qPCR analysis. As presented in Fig. 3A-F, LPS significantly increased the levels of inflammatory factors compared with the control group, including TNF-α, IL-6 and

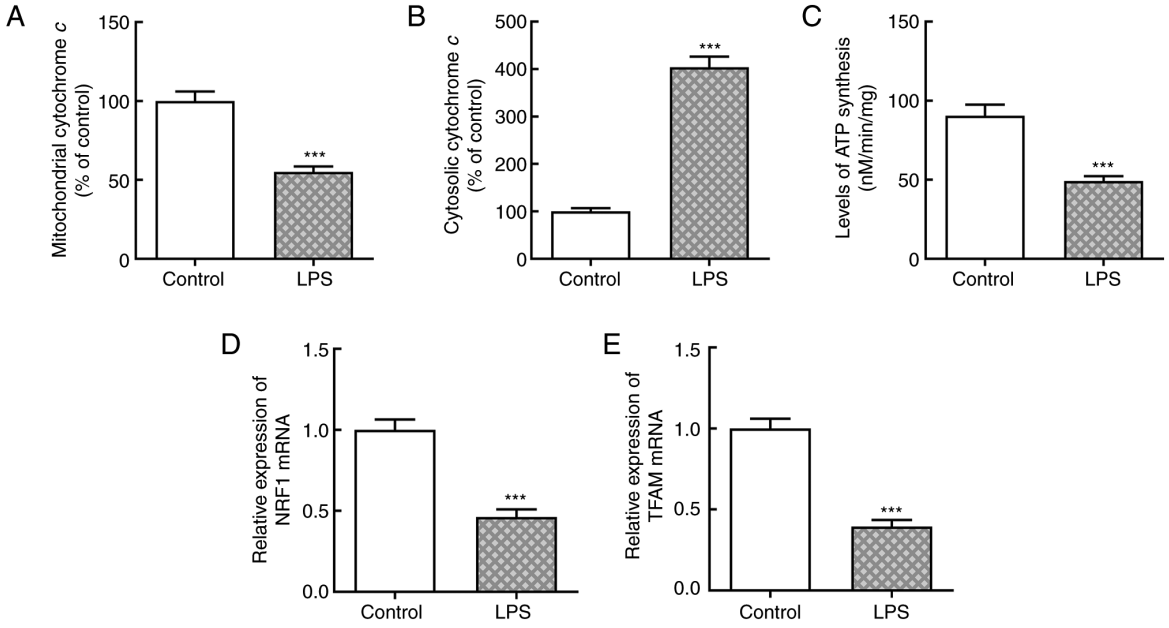

Figure 1. LPS induces mitochondrial dysfunction in AML12 cells. The contents of (A) mitochondrial and (B) cytosolic cytochrome *c* were measured using corresponding kits. (C) ATP synthesis was evaluated via the luciferin-luciferase reaction. The relative mRNA expression levels of (D) NRF1 and (E) TFAM were detected using reverse transcription-quantitative PCR analysis. Cells were treated with LPS (100 ng/ml). ***P<0.001 vs. control. LPS, lipopolysaccharide; NRF1, nuclear respiratory factor 1; TFAM, transcription factor A, mitochondrial.

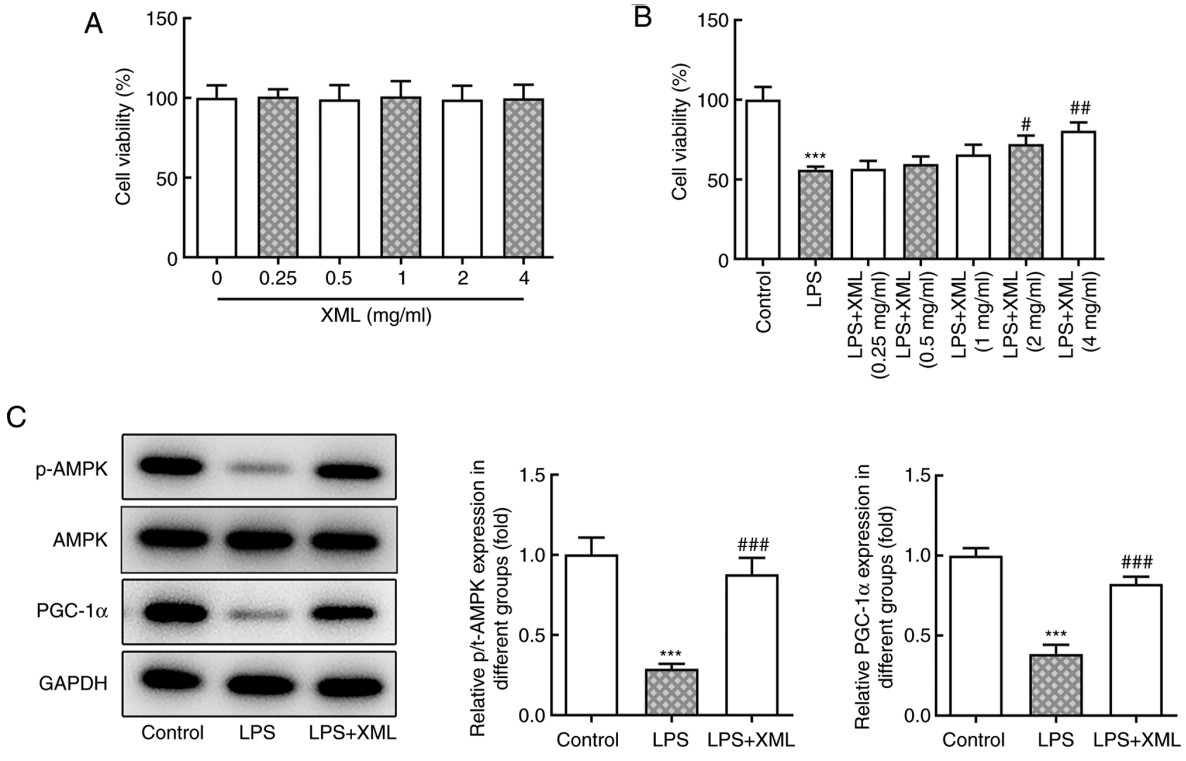

Figure 2. XML treatment activates the AMPK/PGC-1α signaling pathway in LPS-stimulated AML12 cells. (A) MTT assay was used to detect the viability of AML12 cells treated with different concentrations of XML (0.25, 0.5, 1, 2 and 4 mg/ml). (B) MTT assay was used to examine the effect of different concentrations of XML (0.25, 0.5, 1, 2 and 4 mg/ml) on the viability of 100 ng/ml LPS-induced AML12 cells. (C) Western blot analysis was performed to detect the expression levels of proteins in the AMPK/PGC-1α signaling pathway in 100 ng/ml LPS-induced AML12 cells after 4 mg/ml XML treatment. ***P<0.001 vs. control; #P<0.01, ##P<0.01, ###P<0.001 vs. LPS. XML, xinmailong; AMPK, AMP-activated protein kinase; PGC-1α, proliferator-activated receptor γ coactivator-1α; LPS, lipopolysaccharide; p, phosphorylated; t, total.

IL-1β, and these levels were significantly decreased following treatment with XML. Notably, combined treatment with XML and compound C increased the expression levels of these factors compared with the LPS+XML group (Fig. 3A-F). In addition, LPS induction significantly elevated the content of MDA, accompanied by significantly decreased SOD activity,

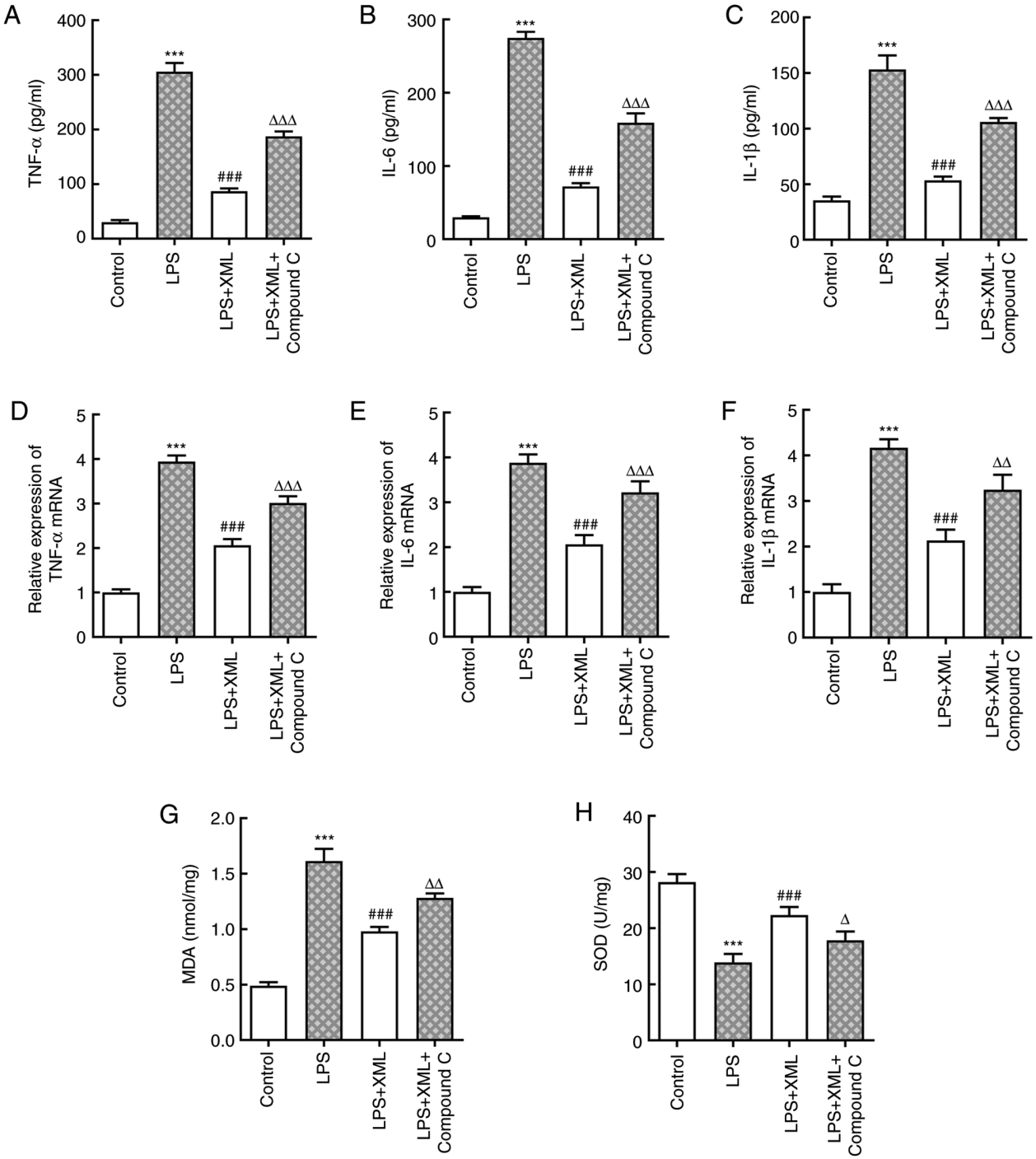

Figure 3. XML treatment suppresses LPS-induced inflammation and oxidative stress in AML12 cells via the activation of AMP-activated protein kinase/proliferator-activated receptor γ coactivator-1α signaling. Levels of (A) TNF-α, (B) IL-6 and (C) IL-β were detected using commercial ELISA kits. mRNA expression levels of (D) TNF-α, (E) IL-6 and (F) IL-β were determined using reverse transcription-quantitative PCR. Levels of (G) MDA and (H) SOD were evaluated using corresponding kits. LPS, 100 ng/ml; XML, 4 mg/ml; compound C, 2 mg/ml. ***P<0.001 vs. control; $^{###}$P<0.001 vs. LPS; ^{Δ}P<0.05, ^{ΔΔ}P<0.01, ^{ΔΔΔ}P<0.001 vs. LPS+XML. XML, xinmailong; LPS, lipopolysaccharide; MDA, malondialdehyde; SOD, superoxide dismutase.

compared with the group without LPS; these effects were attenuated following treatment with XML compared with the LPS treatment group. Furthermore, compound C intervention reversed the effect of XML on oxidative stress (Fig. 3G and H). The results of the TUNEL assay further demonstrated the ability of XML to inhibit the apoptosis of LPS-induced AML12 cells, as the apoptosis of AML12 cells triggered by LPS decreased in the LPS+XML group compared with the LPS intervention group (Fig. 4A and B). However, the LPS+XML+compound C group exhibited a higher apoptotic rate compared with the LPS+XML group. The expression of apoptosis-related proteins determined via western blot analysis exhibited a similar trend (Fig. 4C). Collectively, these results suggested that XML may suppress LPS-induced liver injury by activating the AMPK/PGC-1α signaling pathway.

XML suppresses mitochondrial dysfunction induced by LPS by activating AMPK/PGC-1α signaling in AML12 cells. Liver

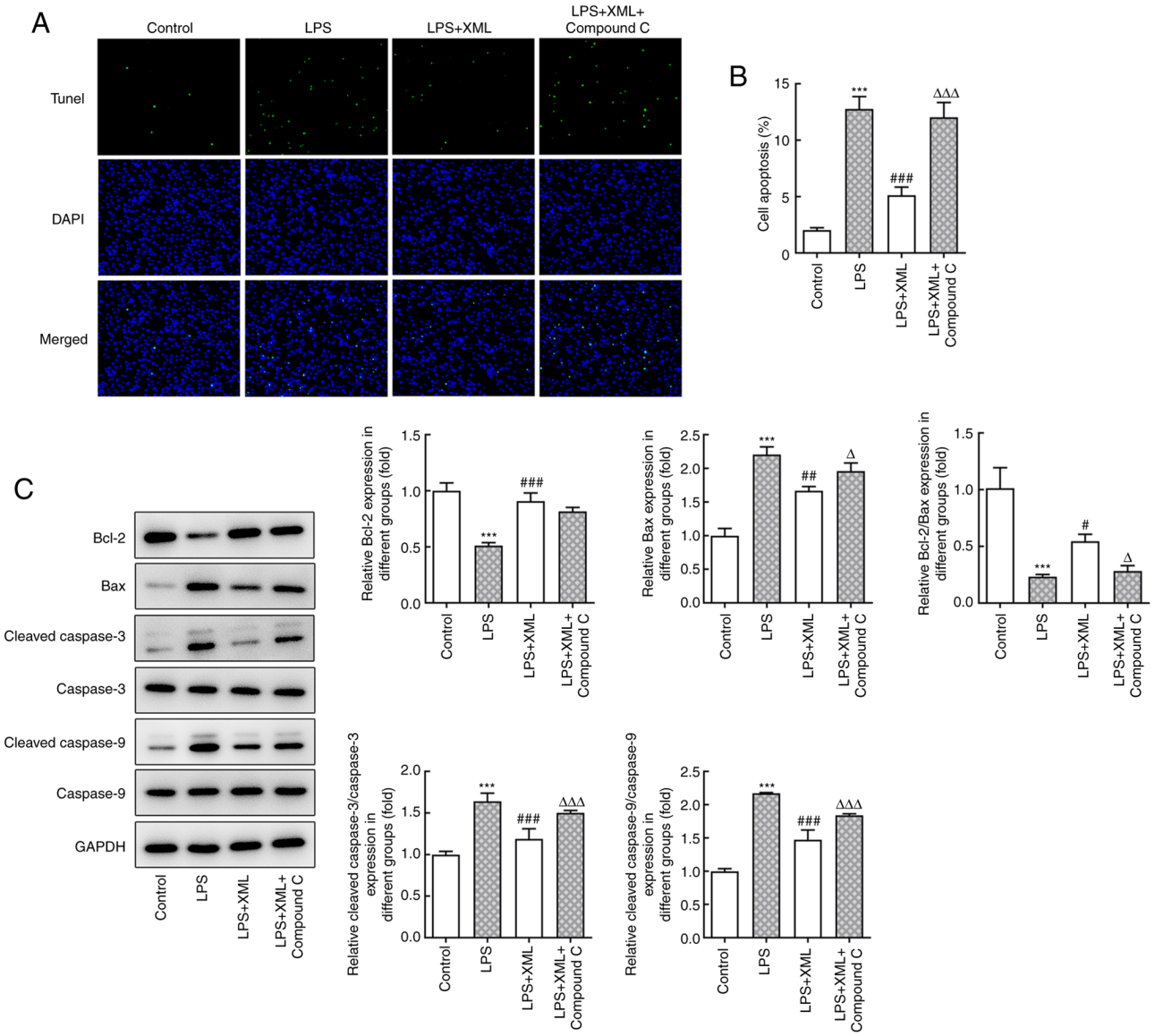

Figure 4. XML treatment attenuates the cell apoptosis of LPS-induced AML12 cells. (A) Apoptosis of AML12 cells was determined using a TUNEL assay. (B) Quantification of cell apoptosis. (C) Western blot analysis was employed to assess the expression of apoptosis-related proteins. LPS, 100 ng/ml; XML, 4 mg/ml; compound C, 2 mg/ml. ***P<0.001 vs. control; $^{\#}$P<0.05, $^{\#\#}$P<0.01, $^{\#\#\#}$P<0.001 vs. LPS; $^{\Delta}$P<0.05, $^{\Delta\Delta\Delta}$P<0.001 vs. LPS+XML. XML, xinmailong; LPS, lipopolysaccharide.

dysfunction is manifested by mitochondrial dysfunction, and mitochondrial dysfunction and cellular energy depletion enhance acute liver injury induced by sepsis (18,19). Thus, it was hypothesized that XML may suppress mitochondrial dysfunction induced by LPS by activating the AMPK/PGC-1α signaling pathway, thereby resulting in the alleviation of hepatocellular injury induced by LPS. LPS significantly decreased the content of mitochondrial cytochrome *c* and significantly increased the content of cytosolic cytochrome *c* compared with the untreated group, and these effects were reversed following treatment with XML (Fig. 5A and B). However, the addition of compound C significantly increased cytosolic cytochrome *c* content compared with the LPS+XML group and decreased in mitochondrial cytochrome *c* content, although this was not statistically significant (Fig. 5A and B). The synthesis of ATP, reduced by LPS, was significantly enhanced following treatment with XML compared with the LPS group, which was reversed by compound C (Fig. 5C). The mRNA expression levels of NRF1 and TFAM were detected via RT-qPCR analysis. As presented in Fig. 5D and E, LPS significantly downregulated the expression levels of NRF1 and TFAM, which was abrogated following treatment with XML. Furthermore, compound C markedly downregulated the expression levels of NRF1 and TFAM compared with the LPS+XML group. Collectively, these results indicated that XML may suppress mitochondrial dysfunction induced by LPS by activating the AMPK/PGC-1α signaling pathway.

Discussion

PA extract is reported to exert therapeutic effects in various diseases, such as fever, inflammation and chronic heart failure (20). Furthermore, the bioactive compounds of PA extract exert anti-inflammatory, antipyretic, antioxidant and

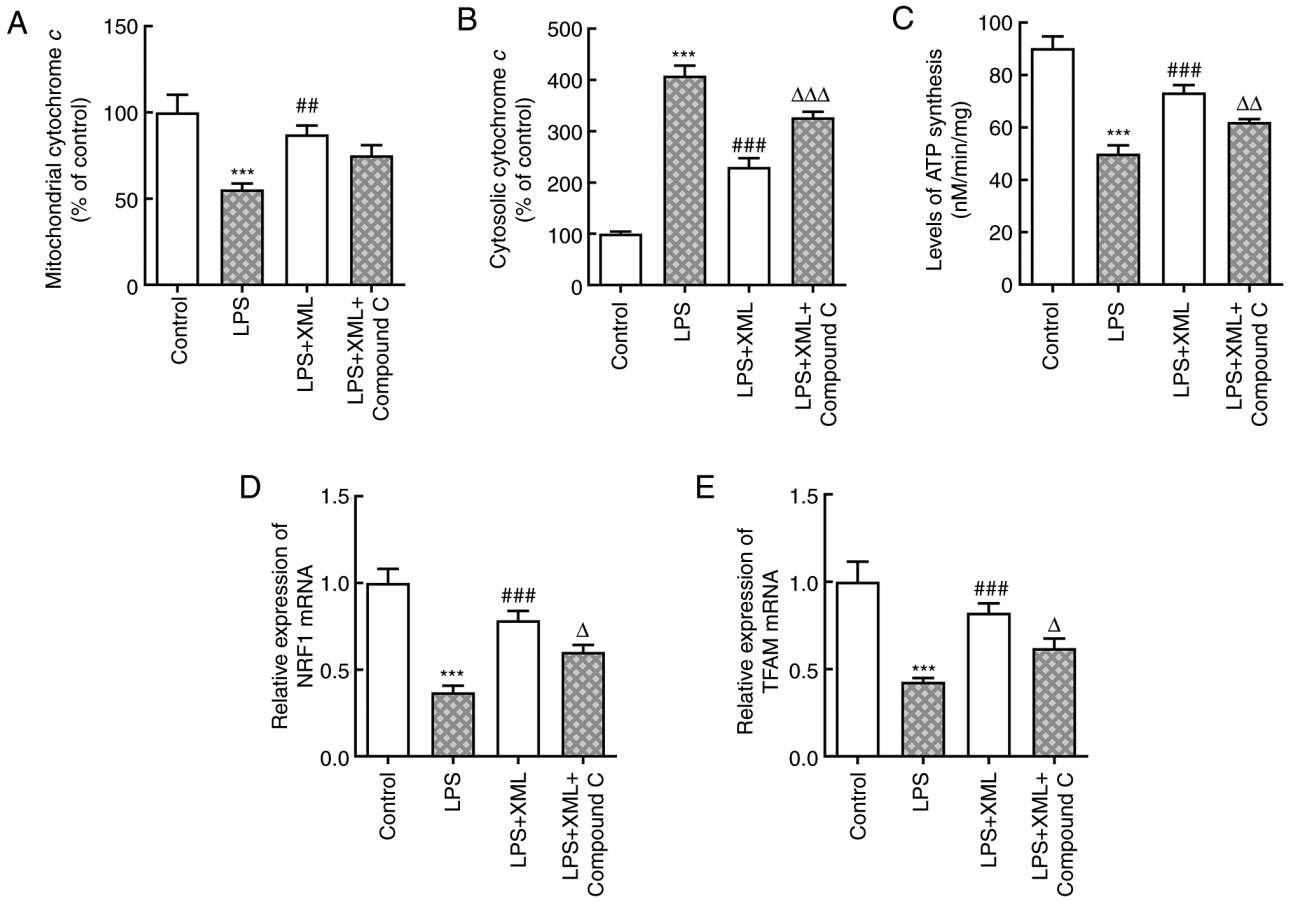

Figure 5. XML suppresses the mitochondrial dysfunction induced by LPS via the activation of AMP-activated protein kinase/proliferator-activated receptor γ coactivator-1α signaling in AML12 cells. Contents of (A) mitochondrial and (B) cytosolic cytochrome *c* were measured using corresponding kits. (C) Synthesis of ATP was evaluated using a luciferin-luciferase reaction. The relative mRNA levels of (D) NRF1 and (E) TFAM were detected using reverse transcription-quantitative PCR. LPS, 100 ng/ml; XML, 4 mg/ml; compound C, 2 mg/ml. ***P<0.001 vs. control; $^{\#\#}$P<0.01, $^{\#\#\#}$P<0.001 vs. LPS; $^{\Delta}$P<0.05, $^{\Delta\Delta}$P<0.01, $^{\Delta\Delta\Delta}$P<0.001 vs. LPS+XML. XML, xinmailong; LPS, lipopolysaccharide; NRF1, nuclear respiratory factor 1; TFAM, transcription factor A, mitochondrial.

analgesic effects by suppressing the MAPK/NF-κB signaling pathway (20). Previous reports have also indicated the significance of PA extract in immune enhancement, wound healing, anti-fibrosis and protection against viral infections (12,13,21). Additionally, PA extract attenuated gastrointestinal complications, and improved immune function and nutritional status in patients with systemic inflammatory response syndrome (12). Of note, PA extract accelerated liver regeneration in a mouse liver regeneration model following 70% partial hepatectomy and a hepatocyte culture via a complex network of pathways, including the AMPK signaling pathway (14). However, the beneficial effects and mechanisms underlying PA extract in sepsis-induced hepatocyte injury remain to be elucidated. The present study utilized XML and established an LPS-induced liver injury model *in vitro* to determine the underlying molecular mechanism. The results demonstrated that XML ameliorated LPS-induced hepatocyte damage by improving mitochondrial dysfunction via the AMPK/PGC-1α signaling pathway.

Mitochondrial dysfunction leads to an impairment of fat homeostasis and overproduction of reactive oxygen species in the liver, which play important roles in the promotion of liver injury (22,23). LPS induces ATP deficiency in mitochondria, resulting in cellular dysfunction and cell death (24). The promoter of cytochrome *c* comprises a recognition site for the transcription factor NRF1, which is responsible for the regulation of the expression of genes involved in the respiratory chain. Furthermore, NRF1 has the ability to activate TFAM (25,26). In the present study, the translocation of mitochondrial cytochrome *c* to the cytoplasm, a decrease in ATP levels and decreased mitochondrial gene expression demonstrated the presence of mitochondrial dysfunction in AML12 cells.

The degradative products of cells are eliminated by a process referred to as autophagy (27). Autophagy maintains cellular homeostasis, while imbalance in the level of autophagy is associated with tissue injury, cancer and liver-related diseases (28). Mitophagy, a specific type of autophagy that removes damaged mitochondria, restrains mitochondrial dysfunction triggered by oxidative stress and decreases the accumulation of mutations in mitochondrial DNA (29). Defects in mitophagy incur mitochondrial dysfunction under conditions of liver injury induced by ischemic reperfusion (30). The regulation of autophagy is a complex process involving various signaling pathways, including the AMPK-mediated signaling pathway (31,32). AMPK indirectly facilitates mitophagy and cell survival (33). In the present study, the role of XML in the AMPK/PGC-1α signaling pathway was investigated.

AMPK is a key regulator of mitochondrial biogenesis, and the downstream effector of AMPK, PGC-1α, is required to

increase the expression of genes associated with oxidative stress following AMPK activation (34). PGC-1α is a potent stimulator that promotes the biogenesis of mitochondria and transcription of genes in the liver, heart and skeletal muscle (35). Under conditions such as fasting and physical exertion, where energy is lacking or in demand, PGC-1α is induced or activated (36). In addition, the regulation of PGC-1α by AMPK is crucial for the modulation of mitochondrial biogenesis (37). In the present study, the suppression of AML12 cell viability by LPS was alleviated by increasing the concentration of XML. The expression levels of p-AMPK and PGC-1α increased following addition of XML to LPS-induced AML12 cells, suggesting that XML activates the AMPK/PGC-1α signaling pathway. Thus, it was hypothesized that XML exerts inhibitory effects on LPS-induced liver injury via the AMPK/PGC-1α signaling pathway. The results of the functional experiments confirmed that XML alleviated the effects on LPS-induced liver injury, as inflammation- and oxidative stress-related factors decreased following treatment of AML12 cells with XML, the effects of which were reversed following treatment with compound C. In addition, compound C promoted the apoptosis of AML12 cells. There is a close association between mitochondrial dysfunction and liver injury, and the results of the present study demonstrated that XML suppressed mitochondrial dysfunction induced by LPS by activating the AMPK/PGC-1α signaling pathway.

In conclusion, the results of the present study demonstrated that XML suppressed mitochondrial dysfunction induced by LPS by activating the AMPK/PGC-1α signaling pathway, which may contribute to understanding of the underlying mechanism via which XML alleviates liver injury.

Acknowledgements

Not applicable.

Funding

The present study was supported by Traditional Chinese Medicine Science and Technology Development Program of Jiangsu Province (grant no. YB201991).

Availability of data and materials

The datasets used and/or analyzed during the current study are available from the corresponding author on reasonable request.

Authors' contributions

WS and JL were responsible for conceiving and designing the study. WS, LA, JZ and JL performed the experiments. WS, LA and JL analyzed the data and reviewed the manuscript. WS, LA and JZ were responsible for drafting the manuscript. JL interpreted data and revised the final manuscript. All authors have read and approved the final manuscript. WS, LA, JZ and JL confirm the authenticity of all the raw data.

Ethics approval and consent to participate

Not applicable.

Patient consent for publication

Not applicable.

Competing interests

The authors declare that they have no competing interests.

References

1. Trefts E, Gannon M and Wasserman DH: The liver. Curr Biol 27: R1147-R1151, 2017.
2. Miyajima A, Tanaka M and Itoh T: Stem/progenitor cells in liver development, homeostasis, regeneration, and reprogramming. Cell Stem Cell 14: 561-574, 2014.
3. Strnad P, Tacke F, Koch A and Trautwein C: Liver-guardian, modifier and target of sepsis. Nat Rev Gastroenterol Hepatol 14: 55-66, 2017.
4. Angus DC, Linde-Zwirble WT, Lidicker J, Clermont G, Carcillo J and Pinsky MR: Epidemiology of severe sepsis in the United States: Analysis of incidence, outcome, and associated costs of care. Crit Care Med 29: 1303-1310, 2001.
5. Singer M, Deutschman CS, Seymour CW, Shankar-Hari M, Annane D, Bauer M, Bellomo R, Bernard GR, Chiche JD, Coopersmith CM, *et al*: The third international consensus definitions for sepsis and septic shock (sepsis-3). JAMA 315: 801-810, 2016.
6. Savio LEB, de Andrade Mello P, Figliuolo VR, de Avelar Almeida TF, Santana PT, Oliveira SDS, Silva CLM, Feldbrügge L, Csizmadia E, Minshall RD, *et al*: CD39 limits P2X7 receptor inflammatory signaling and attenuates sepsis-induced liver injury. J Hepatol 67: 716-726, 2017.
7. Zhang H, Wei L, Zhang Z, Liu S, Zhao G, Zhang J and Hu Y: Protective effect of *Periplaneta americana* extract on intestinal mucosal barrier function in patients with sepsis. J Tradit Chin Med 33: 70-73, 2013.
8. Zhao Y, Yang A, Tu P and Hu Z: Anti-tumor effects of the American cockroach, *Periplaneta americana*. Chin Med 12: 26, 2017.
9. Li QJ, Wang ZG, Liu Q, Xie Y and Hu HL: Research status of *Periplaneta americana* with analyses and prospects of key issues. Zhongguo Zhong Yao Za Zhi 43: 1507-1516, 2018 (In Chinese).
10. Ma X, Hu Y, Li X, Zheng X, Wang Y, Zhang J, Fu C and Geng F: *Periplaneta americana* ameliorates dextran sulfate sodium-induced ulcerative colitis in rats by Keap1/Nrf-2 activation, intestinal barrier function, and gut microbiota regulation. Front Pharmacol 9: 944, 2018.
11. Li J, Shi W, Zhang J and Ren L: To explore the protective mechanism of PTEN-induced kinase 1 (PINK1)/parkin mitophagy-mediated extract of *Periplaneta americana* on lipopolysaccharide-induced cardiomyocyte injury. Med Sci Monit 25: 1383-1391, 2019.
12. Zhang HW, Wei LY, Zhao G, Yang YJ, Liu SZ, Zhang ZY, Jing Z and Hu YL: *Periplaneta americana* extract used in patients with systemic inflammatory response syndrome. World J Emerg Med 7: 50-54, 2016.
13. Li D, Li W, Chen Y, Liu L, Ma D, Wang H, Zhang L, Zhao S and Peng Q: Anti-fibrotic role and mechanism of *Periplaneta americana* extracts in CCl4-induced hepatic fibrosis in rats. Acta Biochim Biophys Sin (Shanghai) 50: 491-498, 2018.
14. Zou Y, Zhang M, Zeng D, Ruan Y, Shen L, Mu Z, Zou J, Xie C, Yang Z, Qian Z, *et al*: *Periplaneta americana* extracts accelerate liver regeneration via a complex network of pathways. Front Pharmacol 11: 1174, 2020.
15. Xing W, Yang L, Peng Y, Wang Q, Gao M, Yang M and Xiao X: Ginsenoside Rg3 attenuates sepsis-induced injury and mitochondrial dysfunction in liver via AMPK-mediated autophagy flux. Biosci Rep 37: BSR20170934, 2017.
16. Yang Q, Han B, Xue J, Lv Y, Li S, Liu Y, Wu P, Wang X and Zhang Z: Hexavalent chromium induces mitochondrial dynamics disorder in rat liver by inhibiting AMPK/PGC-1α signaling pathway. Environ Pollut 265: 114855, 2020.
17. Livak KJ and Schmittgen TD: Analysis of relative gene expression data using real-time quantitative PCR and the 2(-Delta Delta C(T)) method. Methods 25: 402-408, 2001.
18. Singer M: The role of mitochondrial dysfunction in sepsis-induced multi-organ failure. Virulence 5: 66-72, 2014.

19. Yan J, Li S and Li S: The role of the liver in sepsis. Int Rev Immunol 33: 498-510, 2014.
20. Nguyen T, Chen X, Chai J, Li R, Han X, Chen X, Liu S, Chen M and Xu X: Antipyretic, anti-inflammatory and analgesic activities of *Periplaneta americana* extract and underlying mechanisms. Biomed Pharmacother 123: 109753, 2020.
21. Alcantara-Neves NM, Veiga RV, Ponte JC, da Cunha SS, Simões SM, Cruz ÁA, Yazdanbakhsh M, Matos SM, Silva TM, Figueiredo CA, *et al*: Dissociation between skin test reactivity and anti-aeroallergen IgE: Determinants among urban Brazilian children. PLoS One 12: e0174089, 2017.
22. Chen P, Shen Y, Shi H, Ma X, Lin B, Xiao T, Wu F, Zhu J, Li Z, Xiao J, *et al*: Gastroprotective effects of kangfuxin-against ethanol-induced gastric ulcer via attenuating oxidative stress and ER stress in mice. Chem Biol Interact 260: 75-83, 2016.
23. Song Q, Xie Y, Gou Q, Guo X, Yao Q and Gou X: JAK/STAT3 and smad3 activities are required for the wound healing properties of *Periplaneta americana* extracts. Int J Mol Med 40: 465-473, 2017.
24. Paradies G, Paradies V, Ruggiero FM and Petrosillo G: Oxidative stress, cardiolipin and mitochondrial dysfunction in nonalcoholic fatty liver disease. World J Gastroenterol 20: 14205-14218, 2014.
25. Kelly DP and Scarpulla RC: Transcriptional regulatory circuits controlling mitochondrial biogenesis and function. Genes Dev 18: 357-368, 2004.
26. Evans MJ and Scarpulla RC: Interaction of nuclear factors with multiple sites in the somatic cytochrome *c* promoter. Characterization of upstream NRF-1, ATF, and intron Sp1 recognition sequences. J Biol Chem 264: 14361-14368, 1989.
27. Levine B, Packer M and Codogno P: Development of autophagy inducers in clinical medicine. J Clin Invest 125: 14-24, 2015.
28. Doria A, Gatto M and Punzi L: Autophagy in human health and disease. N Engl J Med 368: 1845, 2013.
29. Pickles S, Vigié P and Youle RJ: Mitophagy and quality control mechanisms in mitochondrial maintenance. Curr Biol 28: R170-R185, 2018.
30. Kim JS, Nitta T, Mohuczy D, O'Malley KA, Moldawer LL, Dunn WA Jr and Behrns KE: Impaired autophagy: A mechanism of mitochondrial dysfunction in anoxic rat hepatocytes. Hepatology 47: 1725-1736, 2008.
31. Li Y and Chen Y: AMPK and autophagy. Adv Exp Med Biol 1206: 85-108, 2019.
32. Glick D, Barth S and Macleod KF: Autophagy: Cellular and molecular mechanisms. J Pathol 221: 3-12, 2010.
33. Egan DF, Shackelford DB, Mihaylova MM, Gelino S, Kohnz RA, Mair W, Vasquez DS, Joshi A, Gwinn DM, Taylor R, *et al*: Phosphorylation of ULK1 (hATG1) by AMP-activated protein kinase connects energy sensing to mitophagy. Science 331: 456-461, 2011.
34. Bergeron R, Ren JM, Cadman KS, Moore IK, Perret P, Pypaert M, Young LH, Semenkovich CF and Shulman GI: Chronic activation of AMP kinase results in NRF-1 activation and mitochondrial biogenesis. Am J Physiol Endocrinol Metab 281: E1340-E1346, 2001.
35. Jäger S, Handschin C, St-Pierre J and Spiegelman BM: AMP-activated protein kinase (AMPK) action in skeletal muscle via direct phosphorylation of PGC-1alpha. Proc Natl Acad Sci USA 104: 12017-12022, 2007.
36. Gerhart-Hines Z, Rodgers JT, Bare O, Lerin C, Kim SH, Mostoslavsky R, Alt FW, Wu Z and Puigserver P: Metabolic control of muscle mitochondrial function and fatty acid oxidation through SIRT1/PGC-1alpha. EMBO J 26: 1913-1923, 2007.
37. Reznick RM, Zong H, Li J, Morino K, Moore IK, Yu HJ, Liu ZX, Dong J, Mustard KJ, Hawley SA, *et al*: Aging-associated reductions in AMP-activated protein kinase activity and mitochondrial biogenesis. Cell Metab 5: 151-156, 2007.